Int. J. Mol. Sci. **2000**, *1*, 28-38

International Journal of
Molecular Sciences
ISSN 1422-0067

www.mdpi.org/ijms/

Magnitude of the First and Second Neighbour Magnetic Interactions in the Spin Chain Compound Li_2CuO_2

C. de Graaf*, I. de P. R. Moreira and F. Illas

Dept. de Química Física i Centre Especial de Recerca en Química Teòrica, Universitat de Barcelona, C/ Martí i Franquès 1, 08028 Barcelona, Spain
Tel.: +34-934029021, Fax: +34-934021231, E-mail: c.degraaf@qf.ub.es, f.illas@qf.ub.es

Received: 5 July 2000 / Accepted: 21 August 2000 / Published: 23 August 2000

Abstract: State-of-the-art molecular quantum chemical techniques have been applied to the solid-state compound Li_2CuO_2 in order to derive accurate estimates of the in-chain magnetic interactions. In the present work, the magnitude of the nearest neighbour and next nearest neighbour magnetic coupling constants is investigated from first principles embedded cluster calculations. The convergence of the results is carefully tested for the cluster size. In contrast to the earlier findings, it is predicted that J_2 is only ~15% of J_1. In particular, it is shown that a large J_2 appears when the Li^+ ions are not explicitly included in the calculation.

Keywords: magnetic interactions, cluster model approach, difference dedicated CI, CASPT2, Li_2CuO_2

1. Introduction

The nature and magnitude of the magnetic interactions between copper ions in the cuprates are largely dependent on the way in which the characteristic CuO_4 squares are linked together. According to the Goodenough-Kanamori-Anderson (GKA) rules [1-3], the first neighbour interaction varies from strongly antiferromagnetic in the case of linear Cu–O–Cu bonds to weakly ferromagnetic for Cu–O–Cu bond angles of 90°. Corner sharing CuO_4 squares are found in the high T_c superconductors and their undoped parent compounds. The size of the first neighbour interaction within the CuO_2 planes is well established. For example in La_2CuO_4 this coupling is considered to be characterized accurately by a J of -135 meV, consistent with the GKA rules. The spin S=1/2 chains found in Sr_2CuO_3 and Ca_2CuO_3 are also formed by corner sharing CuO_4 squares. However, for these compounds the situation is less clear; very different estimates of the first neighbour in-chain interaction have been reported, ranging from -100 to -250 meV [4-7]. Both edge sharing and corner sharing CuO_4 squares are found in many cuprates. An interesting example is the $Sr_{n-1}Cu_nO_{2n-1}$ series of spin ladders. In the Cu_2O_3 planes, corner sharing squares form n-leg ladders and edge sharing squares link the ladders together. The interaction

between the ladders is found to be rather small and ferromagnetic, whereas the intraladder couplings are large and antiferromagnetic, although the relative magnitudes of the coupling along rung and leg are controversial [8, 9].

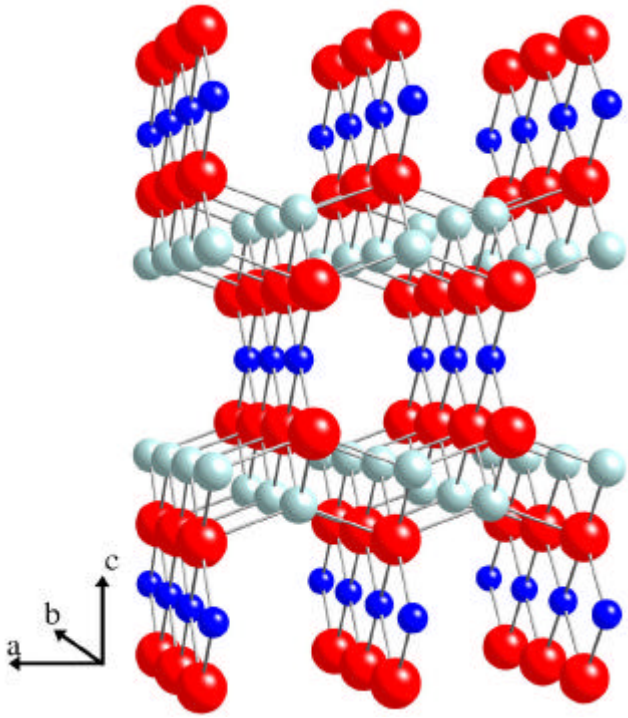

Figure 1. Crystal structure of Li_2CuO_2. Dark blue spheres represent copper ions, red spheres are used for oxygen and light blue spheres depict lithium.

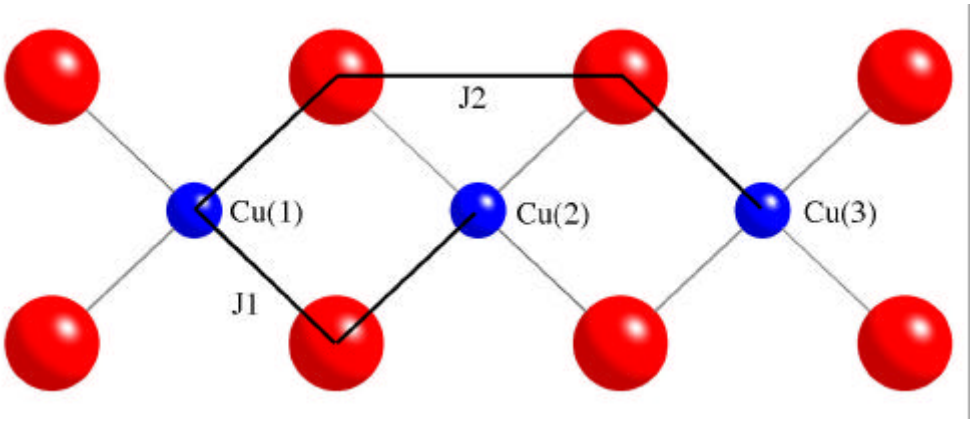

Figure 2. The nearest neighbour interaction path (J_1) and the second nearest neighbour interaction path (J_2) indicated by thicker black lines. Dark blue spheres represent copper ions and red spheres are used to depict oxygens.

Li_2CuO_2 is yet another compound with CuO_4 squares as building blocks. The squares are edge sharing and form spin chains in the b direction of the crystal (see Figure 1 and 2). Figure 2 illustrates the different pathways of the two magnetic in-chain interactions. The GKA rules predict that the first neighbour in-chain magnetic coupling (J_1) is rather weak and ferromagnetic, and in addition, it is expected that the second neighbour interaction (J_2) is of minor importance. However, several articles have been published that consider the magnitude of these couplings and very surprising conclusions were drawn. It is suggested that J_1 is not necessarily ferromagnetic because of the not exactly rectan-

gular Cu–O–Cu angle, which is in fact 94° [10-12]. Mizuno *et al.* [11] derive from a three band Hubbard model that the second neighbour interaction (J_2) is about 60% of J_1 and Weht and Pickett [13] report that J_1 is even larger than J_2. The estimates of J_1 and J_2 are derived from hopping parameters ($J \sim t^2/U$) calculated within the LDA framework. Such a large J_2 value is explained by the short distance between oxygens on the chains which can cause a relatively large overlap between oxygens that connect second neighbour copper ions. Boehm *et al.* [12] study the three dimensional magnetic structure by inelastic neutron scattering. The data are fitted with six different J-values, two in-chain (J_1 and J_2) and four different interchain couplings. They arrive at a very small (-0.24 meV) antiferromagnetic first neighbour interaction and a ferromagnetic second neighbour interaction, which is of the same order of magnitude (0.16 meV) as J_1. In short, there seems to be no consensus about the nature and the magnitude of the different in-chain interactions and moreover, some of the estimates reported in the literature are contradictory to the GKA rules and should be carefully examined.

2. Computational strategy

The present work reports first principles estimates of the magnetic interaction parameters J_1 and J_2 by using theoretical procedures that have been recently shown to quantitatively predict the magnitude of the magnetic coupling constants in a rather large family of ionic insulators [14]. We model the crystal by different clusters and approximate the eigenfunctions of the exact non-relativistic Hamiltonian within the chosen material model by modern quantum chemical techniques. This allows for an accurate treatment of the large electron correlation effects characteristic of the cuprates. The cluster model is validated by an extensive cluster size study. Furthermore, we study the convergence of J with the basis set. The basic cluster is a Cu_3O_8 unit with D_{2h} symmetry, i.e. three copper ions on a chain extended with their neighbouring oxygen ions (as shown in Figure 2). This cluster allows for a simultaneous calculation of the first and second neighbour interaction using the relations between the spin eigenstates of the Heisenberg Hamiltonian, $\hat{H} = -J_1(\hat{S}_1 \hat{S}_2 + \hat{S}_2 \hat{S}_3) - J_2 \hat{S}_1 \hat{S}_3$, and the electronic eigenstates of the Hamiltonian of the material model. From the mapping of the energy eigenvalues of the electronic eigenstates onto the Heisenberg Hamiltonian, we obtain: $J_1 = 2/3\ (\ E(^2B_{1u}) - E(^4B_{1u})\ )$ and $J_2 = J_1 - (\ E(^2B_{1u}) - E(^2B_{3g})\ )$. In addition we define two clusters with only two copper ions. The first is a Cu_2O_6 cluster from which we calculate J_1 and the second is a Cu_2O_8 cluster to extract J_2. This latter cluster is the same as shown in Figure 1, with the central Cu replaced by a 2+ point charge, and hence, basically the second neighbour interaction is present. For the two centre clusters, J is obtained from the energy difference of the triplet and the singlet eigenstate of the electronic Hamiltonian. We refer the reader to previous work [15, 16] for a more comprehensive description of the mapping procedures between the eigenstates of the electronic cluster Hamiltonian and the Heiesenberg Hamiltonian.

3. Methods

The structure of Li_2CuO_2 is taken from experiment [10], and is the only input external to theory. The Cu–O distance is 1.956 Å, the Cu–Cu distance and the O–O distance along the chains is 2.860 Å. For comparison, the interatomic distance for oxygens in corner sharing chain compounds as Sr_2CuO_3 and Ca_2CuO_3 is 3.9 Å. The three clusters are embedded in a set of point charges that represent the Madelung potential in the whole cluster region. To avoid a spurious polarization of the cluster charge

density towards the point charges, the copper ions closest to the cluster are represented by total ion potentials (TIPs) [17]. The cluster ions are described at an all-electron level with the following gaussian-type orbital basis sets: Cu (5s,4p,3d), the bridging oxygens (4s, 3p) and the edge O (3s,2p) [18, 19]. Although this somewhat rough representation of the material already gives reasonable results, a significant improvement can be obtained by replacing a larger number of point charges near the cluster by model potentials, including in this way the short range repulsion between the cluster ions and the direct cluster environment. The ions closest to the cluster are the Li^+ ions in the b-c plane. Because of the limited number of electrons associated with the Li^+ ions, we treat them as all electron ions with a (2s) basis set. For the Cu_2O_6 cluster four lithiums are added, for the other clusters we add six ions.

The electronic structure calculations are based on two different strategies. The first one is based on the direct calculation of the energy differences between the eigenstates involved starting from a small complete active space configuration interaction (CASCI) wave function as reference. A CI expansion of the N-electron wave function is constructed by selecting only those determinants that up to second-order perturbation theory contribute to the energy difference of the eigenstates of the reference CASCI wave function [20]. The diagonalization of this list substantially improves the energy differences obtained by an (almost) uncorrelated approximation, but it fails to fully repair the overestimation of the on-site repulsion U. Therefore, the list is extended with the determinants connected to the relaxation of the ligand to metal charge transfer configurations in order to allow for a more efficient screening of U. A recent study [14] has shown that this computational scheme, referred to as DDCI3 [21], Difference Dedicated Configuration Interaction, is able to quantitatively reproduce the magnetic interaction parameters in a wide variety of insulators. Because of the relatively high computational demand of DDCI3, we explore the basis set dependency and the cluster size effects of the calculated magnetic interaction parameters with a second computational scheme, namely second-order perturbation theory by means of CASPT2 [22, 23], Complete Active Space second-order Perturbation Theory. This more approximate method takes a complete active space self consistent field (CASSCF) wave function as zeroth-order wave function and accounts for the remaining (mostly dynamical) electron correlation by second-order perturbation theory. The CAS employed in both the CASPT2 and DDCI the calculations contains the magnetic Cu-$3d_{xy}$ orbitals and the unpaired electrons, i.e. two orbitals and two electrons for the two-center clusters, and three orbitals and three electrons for the three center clusters. This choice of active space ensures a qualitatively correct description of the magnetic coupling interaction and is equivalent to the Anderson model of superexchange (for more details see Ref. [16]). A further extension of the active space only leads to modest changes in the calculated values [24, 25].

All calculations are performed with MOLCAS 4 [26] and the CASDI chain of programs [27].

4. Results and Discussion

A. Accurate Determination of J_1 and J_2

Table I lists the calculated magnetic interaction parameters for the different cluster models in the (almost) uncorrelated approximation (CASSCF) and after accounting for the large external electron correlation effects (CASPT2 and DDCI3). In accordance with the GKA rules, the nearest neighbour interaction J_1 calculated in the Cu_2O_6 and Cu_3O_8 clusters is rather small and positive, i.e. ferromagnetic interaction is preferred. The interaction is enhanced by a factor of three by treating the external corre-

lation effects with second-order perturbation theory. The mean field estimate as well as the value corrected for electron correlation effects do not differ in the two centre and the three centre cluster, reflecting that the nearest neighbour interaction is genuinely a two centre interaction and its magnitude is not influenced by collective effects of the extended system as shown in Ref. [14] and [28]. The extension of the cluster with lithium ions does not change the picture derived from the smaller one. The values are slightly increased, as has been observed before in many other applications; replacing the point charges nearest to the cluster by real charge distributions, either by model potentials, frozen ions or real cluster atoms, slightly improves the description of the magnetic interaction, since the artificial polarization of the electrons towards the point charges is (at least partially) removed. DDCI3 only slightly changes the CASPT2 values and gives us the final estimate of the first neighbour interaction of 12.2 eV.

Table 1. First neighbour (J_1) and second neighbour (J_2) magnetic interaction parameters (in meV) for Li_2CuO_2 with different cluster models. CASSCF represents the Anderson model, while CASPT2 and DDCI3 include external electron correlation effects.

Material	CASSCF		CASPT2		DDCI3	
model	J_1	J_2	J_1	J_2	J_1	J_2
Cu_3O_8	3.5	-1.5	11.6	-8.1	10.6	-8.8
$Cu_3O_8Li_6$	3.8	-0.2	13.1	-1.8	12.2	-1.7
Cu_2O_6	3.5	–	11.1	–	13.4	–
$Cu_2O_6Li_4$	3.8	–	12.7	–	15.4	–
Cu_2O_8	–	-1.3	–	-7.9	–	-10.8
$Cu_2O_8Li_6$	–	-0.3	–	-2.3	–	-2.3

The second neighbour interaction calculated with the Cu_2O_8 and Cu_3O_8 clusters, which possess the essential ingredients to describe J_2 but do not include explicitly the effect of the six Li ions near the cluster, is rather similar to the coupling strength obtained by Mizuno *et al.* [11]. With these clusters, we also find that J_2 is antiferromagnetic and about 80% of J_1 after treating the external electron correlation effects. However, by adding the six Li^+ ions closest to the cluster, we observe a drastic change in the magnitude of the second neighbour magnetic interaction parameter. For CASSCF, J_2 drops to less than 10% of J_1 and a decrease is observed of more than 75% for CASPT2, leaving the magnitude of J_2 to only 15% of J_1. Hence, we conclude that the magnetic interaction path (Cu–O–O–Cu) for the second neighbour interaction is obstructed when the Li ions around the cluster are represented by real charge distributions instead of point charges. The DDCI3 calculation confirms this observation and we predict a rather small J_2 of -1.7 meV, which is only 14% of the final *ab initio* estimate for J_1. The strong influence on J_2 of the Li ions is illustrated in Figure 3, which displays the changes in the spin density

caused by adding the six Li ions to the Cu_2O_8 cluster. The fact that J_2 calculated with the two-center cluster is virtually identical to that obtained with the three-center clusters, makes the $Cu_2O_8Li_6$ cluster especially attractive to investigate the dramatic effect of the Li ions on J_2. The figure clearly illustrates that the introduction of the short-range repulsion between the Li ions and the oxygens on the J_2 magnetic path (Cu(1)–O–O–Cu(3)) significantly reduces the spin density along this path to increase it on the Cu ions. Hence, the overlap between the two oxygens decreases and the two copper ions involved in this magnetic interaction are disconnected magnetically. To avoid confusion, we mention that the spin density of the CASSCF wave function on the Li ions is negative, explaining the decrease of the spin density on the Li ions as shown in Figure 3.

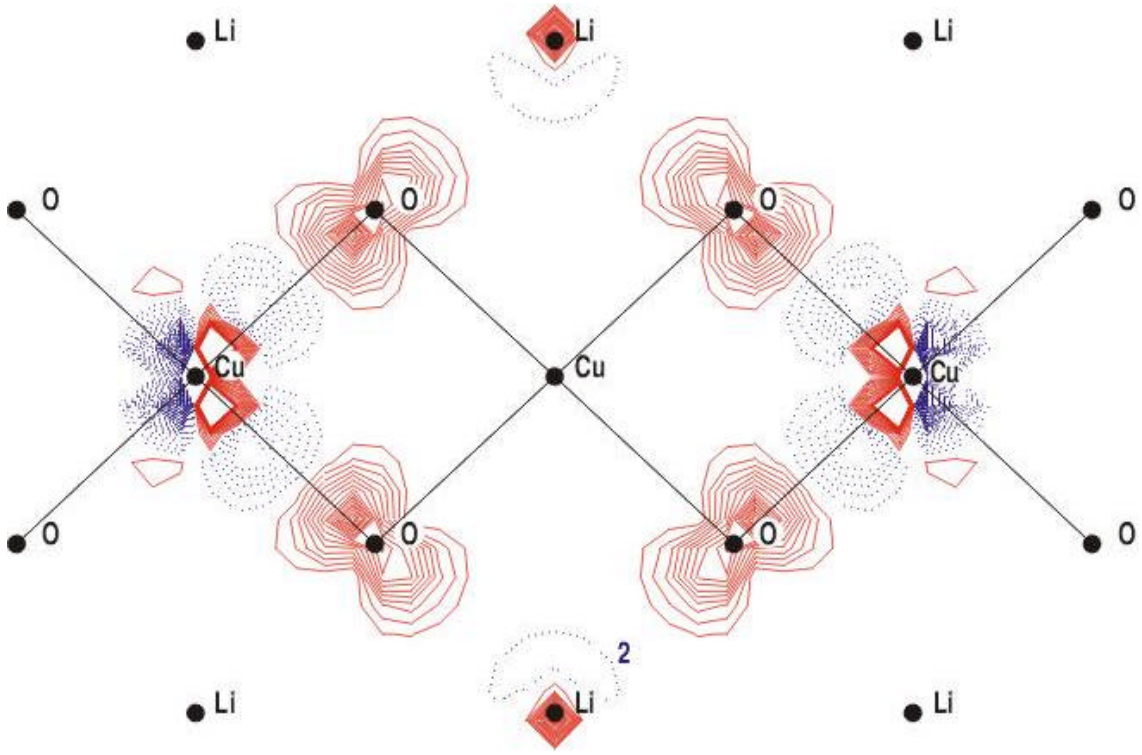

Figure 3. Spin density difference plot of the Cu_2O_8 cluster. The difference is obtained by subtracting the CASSCF spin density of the Cu_2O_8 cluster from the spin density of the $Cu_2O_8Li_6$ cluster. Red contours indicate a reduction of the spin density, while dotted blue contours indicate an increase of the spin density.

It is worth noting that the Li ions only strongly affect J_2 and leave J_1 unchanged. This can be rationalized by the fact that those ions are situated along the magnetic interaction path characterized by J_2. Neither for J_1 nor for magnetic interactions in corner sharing spin chain compounds such a situation exists and therefore the effect of the supplementary ions is much smaller. We conclude that the large J_2 found by Mizuno *et al.* must be ascribed to the fact that the parameters used in the calculations were taken from cuprates that contain corner sharing CuO_4 squares only, and therefore, these effective parameters do not properly include the effect of the supplementary ions as occurs in the present edge sharing compound.

Our calculated values for J_1 and J_2 are larger than the ones derived from experiment by Boehm *et al.* [12] and also somewhat larger than the 1.3 - 2.6 meV estimated for J_1 by fitting high temperature specific heat data [29], but are of the same order of magnitude as the ones calculated by Mizuno *et al.*

[11]. Again, we stress that, although the values are of the same order, the explicit inclusion of the Li ions gives rise to important changes in the ratio of J_1 and J_2.

B. Basis Set and Cluster Size Check

A neccessary check is the dependence of the calculated J's on the basis set size. In Table 3, we report J_1 calculated in the $Cu_2O_6Li_4$ cluster applying five basis sets of different quality. In this series we investigate the effect of the frozen ion description of Li, and the effect of polarization functions on the cluster atoms. The largest basis set considered consists of a (6s, 5p, 4d, 1f) basis for Cu; (5s, 4p, 2d) for O and (3s, 1p) for Li.

The comparison of Basis **A**, **B**, **D** and **E** shows that the values in Table 1 are converged for the size of the basis set. Adding polarization functions and/or any further extension of the basis set on the cluster ions does not change any of the values in the table by more than 0.3 meV. Furthermore, Basis **C** and **D** allow to investigate the role of the Li ions, since these basis sets are equivalent except for the description of the Li ions, in the former being as frozen ions not allowing for any covalent interaction with the oxygens. We conclude that the frozen ion description of the Li ions does not seriously affect the magnitude of the magnetic coupling parameters and that the role of the Li ions is (although essential) completely static.

Table 2. Basis set dependency of the nearest neighbour interaction, J_1 (in meV) calculated in a $Cu_2O_6Li_4$ cluster embedded in two Cu^{2+} TIPS and point charges. Basis **A** consists of the Cu (5s, 4p, 3d) basis, the bridging O (4s, 3p) basis, the edge O (3s, 2p) basis and a Li (2s) basis. Basis **B** augments the edge O basis to (4s, 3p). Basis **C** augments **B** with a d-function on all O but treats the Li ions at the frozen ion level. Basis **D** only differs from **C** in the treatment of the Li ions, namely by a (3s, 1p) basis. Basis **E** consists of a (6s, 5p, 4d, 1f) basis for Cu, a (5s, 4p, 2d) basis for O and a (3s, 1p) basis for Li.

	CASSCF	CASPT2
Basis **A**	3.8	12.7
Basis **B**	3.8	13.0
Basis **C**	4.0	13.7
Basis **D**	3.9	13.0
Basis **E**	3.8	12.7

Still, one can argue that the cluster model provides too crude a representation of the real crystal and that cluster results cannot be trusted. The most straightforward way of testing the models discussed so far is to extend the cluster with more atoms. Starting from the $Cu_2O_6Li_4$ cluster used to extract J_1, successively more shells are added. In a second series of calculations the same strategy is applied for the three-center cluster. The largest cluster we consider is $Cu_2O_6Li_{20}O_{16}Cu_2$ (the two extra Cu ions are represented by TIPs) for the two-centre cluster (see Fig. 3) and $Cu_3O_8Li_{26}0_{12}Cu_2$ in the second series (see Fig 4a and b). Table 3 lists the effects of the increase in the cluster size on the magnetic coupling parameters using Basis **D** for the central cluster atoms ($Cu_2O_6Li_4$ and $Cu_3O_8Li_6$), and (3s, 2p) and (2s) for

the other O and Li ions, respectively. It is readily recognized that this effect is very small, J_1 and J_2 do not significantly depend on the cluster size, provided that the Li ions in the J_2 magnetic pathway are included.

Table 3. Cluster size dependency of the nearest neighbour (J_1) and next-nearest neighbour (J_2) interactions (in meV). All cluster are embedded in two Cu^{2+} TIPS and point charges.

cluster	CASSCF		CASPT2	
	J_1	J_2	J_1	J_2
Cu_2O_6	3.5	–	11.4	–
$Cu_2O_6Li_4$	3.9	–	13.0	–
$Cu_2O_6Li_{20}$	4.1	–	13.2	–
$Cu_2O_6Li_{20}O_{16}$	4.1	–	13.5	–
Cu_3O_8	3.5	-1.5	11.9	-8.5
$Cu_3O_8Li_6$	3.8	-0.3	13.2	-1.9
$Cu_3O_8Li_{10}$	3.9	-0.2	13.3	-1.9
$Cu_3O_8Li_{26}$	4.2	-0.3	14.4	-2.3
$Cu_3O_8Li_{26}O_{12}$	4.1	-0.3	14.1	-2.2

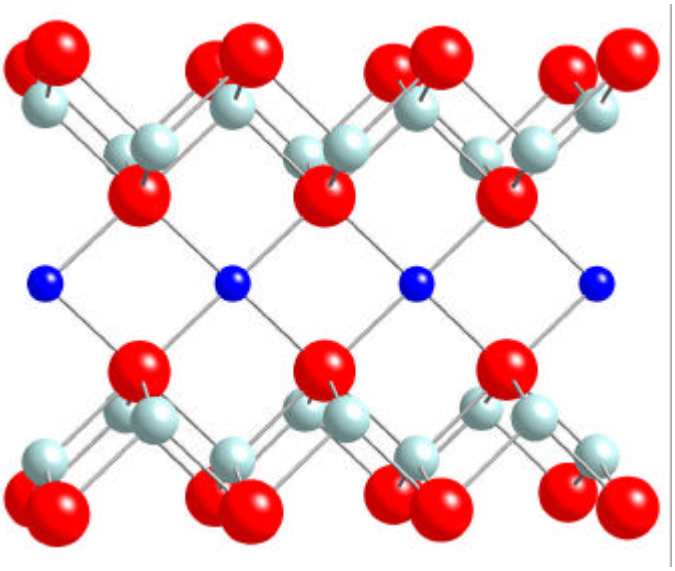

Figure 3. $Cu_2O_6Li_{20}O_{16}Cu_2$ cluster to calculate J_1.

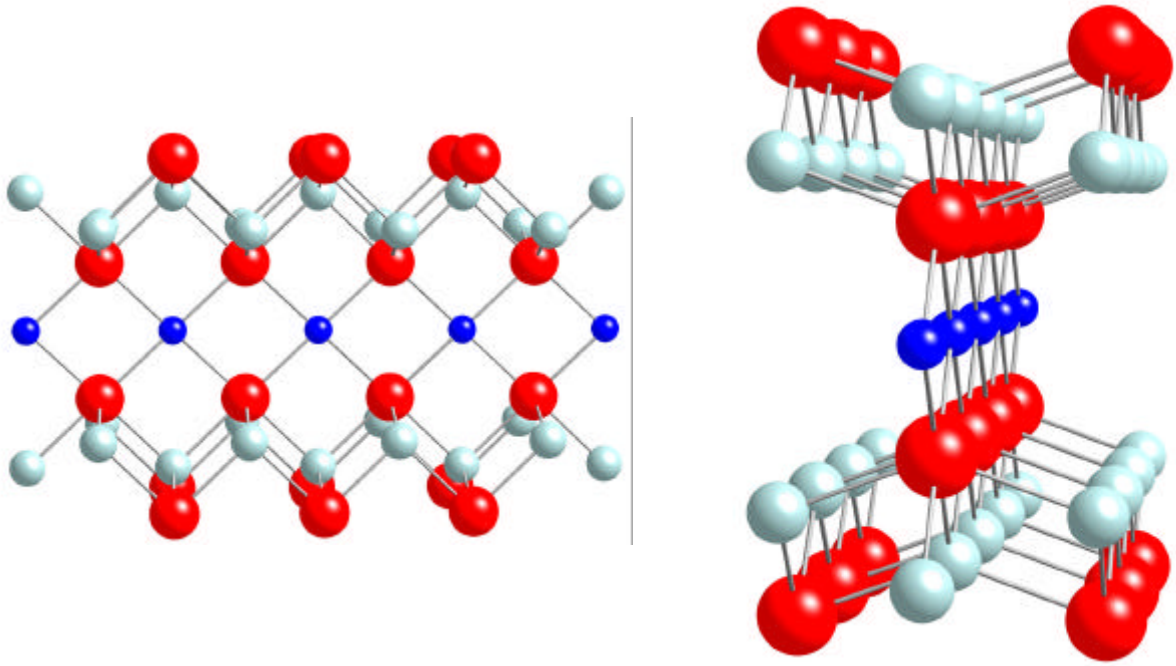

Figure 4. Perpendicular and parallel view of the $Cu_3O_8Li_{26}O_{12}Cu_2$ cluster to calculate J_1 and J_2.

C. Magnetic Moments

Weht and Pickett also claim that Li_2CuO_2 has a magnetic moment associated with oxygen that is larger than for any other transition metal (TM) compound. The total moment per CuO_2 unit is 0.92 μ_B and has been associated completely to the copper ion [10], however, based on LDA calculations, Weht and Pickett associate 60% of the total moment per CuO_2 unit to copper and 40% to oxygen. This leads to a moment for O of almost 0.2 μ_B and for Cu, 0.55 μ_B. The Mulliken spin populations provide a way to extract a measure of the magnetic moment of the different centres from our cluster calculations. The populations of the CASSCF wave function corresponding to the ferromagnetic solution indicate that a very large part of the magnetic moment is concentrated on the Cu ions. In all clusters, we found that the Mulliken spin population of Cu is 0.93, and 0.03 for oxygen. Although the CASSCF wave function includes only a small amount of electron correlation and the way in which the overlap population is divided over the centres –Mulliken population analysis distributes it on equal parts over the two centres involved– is arbitrary, it is clear that our cluster calculations do not support a large spin moment on oxygen ions. The populations have been tested for basis set dependency, but neither smaller nor larger basis sets give rise to significant changes of the values. Moreover, Martin and Illas [30] made a comparison of different density functionals with respect to the magnetic moment derived from the Mulliken spin population for some TM compounds. They observed that LDA significantly underestimates the spin moments on the metal sites. Furthermore, it is well-known that LDA badly fails to reproduce the insulating character of magnetic insulator TM compounds. It is well possible that the large moment reported by Weht and Pickett is an artefact of the LDA method applied to determine the moments.

5. Summary

The study of the magnetic interactions in Li_2CuO_2 by means of *ab initio* cluster models shows that J_1 is ferromagnetic and rather small in magnitude in agreement with the almost rectangular Cu–O–Cu angle. Furthermore we demonstrate that J_2 is not more than 15% of J_1 given that one accounts for the Pauli repulsion of the Li^+ ions closest to the cluster. If not, the overlap of the oxygen charge distributions along the chain is overestimated giving rise to an artificially large J_2. We have carefully checked the dependency of the magnetic coupling parameters on the cluster and basis set size and conclude that the calculated J's are stable against these parameters.

Acknowldgements: Financial support was provided by the "Comisión Interministerial de Ciencia y Tecnología" under CICyT Project No. PB98-1216-CO2-01. C. de G. acknowledges the financial support through the TMR activity "Marie Curie research training grants" Grant No. FMBICT983279 established by the European Community. I. de P. R. M. is grateful to the University of Barcelona for a Ph. D. grant. Partial support from the Generalitat de Catalunya under project 1997SGR00167 is acknowledged.

References and Notes

1. Goodenough, J. B. Theory of the role of covalence in the perovskite-type manganites [La,M(II)] MnO_3. *Phys. Rev.* **1955**, *100*, 564-573.
2. Kanamori, J. *J. Phys. Chem. Solids* **1959**, *10*, 87.
3. Anderson, P. W. *Theory of magnetic exchange interaction: Exchange in insulators and semiconductors*; In *Solid State Physics*; Seitz, F., Turnbull, D., Eds.; Academic Press: New York, 1963; Vol. 14, pp. 99-214.
4. van Oosten, A. B.; Mila, F. Ab initio determination of exchange integrals and Néel temperature in the chain cuprates. *Chem. Phys. Lett.* **1998**, *295*, 359-365.
5. Mizuno, Y.; Tohyama, T.; Maekawa, S. Superexchange interactions in cuprates. *Phys. Rev. B.* **1998**, *58*, 14713-14716.
6. Lorenzana, J.; Eder, R. Dynamics of the one dimensional Heisenberg model and optical absorption of spinons in cuprate antiferromagnetic chains. *Phys. Rev. B.* **1997**, *55*, 3358-3359.
7. Rosner, H.; Eschrig, H.; Hayn, R.; Drechsler, S.-L.; Málek, J. Electronic structure and magnetic properties of the linear chain cuprates Sr_2CuO_3 and Ca_2CuO_3. *Phys. Rev. B.* **1997**, *56*, 3402-3412.
8. de Graaf, C.; de P. R. Moreira, I.; Illas, F.; Martin, R. L. Ab Initio study of the Magnetic Interactions in the Spin Ladder Compound $SrCu_2O_3$. *Phys. Rev. B.* **1999**, *60*, 3457-3464.
9. Sugai, S.; Shinoda, T.; Kobayashi, N.; Hiroi, Z.; Takano, M. Anisotropic exchange integrals in the two-leg spin ladder $LaCuO_{2.5}$. *Phys. Rev. B.* **1999**, *60*, 6969-6972.
10. Sapiña, F.; Rodríguez-Carvajal, J.; Sanchis, M. J.; Ibáñez, R.; Beltrán, A.; Beltrán, D. Crystal and Magnetic Structure of Li_2CuO_2. *Solid Sate Comm.* **1990**, *74*, 779-784.
11. Mizuno, Y.; Tohyama, T.; Maekawa, S.; Osafune, T.; Motoyama, N.; Eisaki, H.; Uchida, S. Electronic states and magnetic properties of edge-sharing Cu - O chains. *Phys. Rev. B.* **1998**, *57*, 5326-5335.
12. Boehm, M.; Coad, S.; Roessli, B.; Zheludev, A.; Zolliker, M.; Böni, P.; Paul, D. M.; Eisaki, H.; Motoyama, N.; Uchida, S. Competing exchange interactions in Li_2CuO_2. *Europhys. Lett.* **1998**, *43*, 77-82.

13. Weht, R.; Pickett, W. E. Extended Moment Formation and Second Neighbor Coupling in Li_2CuO_2. *Phys. Rev. Lett.* **1998**, *81*, 2502-2505.
14. de P. R. Moreira, I.; Illas, F.; Calzado, C. J.; Sanz, J. F.; Malrieu, J.-P.; Ben Amor, N.; Maynau, D. The Local Character of Magnetic Coupling in Ionic Solids. *Phys. Rev. B.* **1999**, *59*, 6593-6596.
15. de P. R. Moreira, I.; Illas, F. Ab Initio theoretical comparative study of magnetic coupling in $KNiF_3$ and K_2NiF_4. *Phys. Rev. B.* **1997**, *55*, 4129-4137.
16. Illas, F.; de P. R. Moreira, I.; de Graaf, C.; Barone, V. Magnetic coupling in biradicals, binuclear complexes and wide gap insulators: A survey of ab initio Wave Function and Density Functional Theory approaches. *Theor. Chem. Acc.* **2000**, *104*, 265-272.
17. Winter, N. W.; Pitzer, R. M.; Temple, D. K. Theoretical study of a Cu^+ ion impurity in a NaF host. *J. Chem. Phys.* **1987**, *86*, 3549-3556.
18. Pou-Amérigo, R.; Merchán, M.; Nebot-Gil, I.; Widmark, P.-O.; Roos, B.O. Density matrix averaged atomic natural orbital (ANO) basis sets for correlated molecular wave functions. *Theor. Chim. Acta.* **1995**, *92*, 149-181.
19. Widmark, P.-O.; Malmqvist, P.-Å.; Roos, B.O. Density matrix averaged atomic natural orbitals (ANO) basis sets for correlated molecular wave functions. I First row atoms. *Theor. Chim. Acta.* **1990**, *77*, 291-306.
20. Malrieu, J.-P. Cancellations occurring in the calculation of transition energies by a perturbation development of Configuration Interaction Matrices. *J. Chem. Phys.* **1967**, *47*, 4555-4558.
21. Miralles, J.; Castell, O.; Caballol, R.; Malrieu, J.-P. Specific CI calculation of energy differences: transition energies and bond energies. *Chem. Phys.* **1993**, *172*, 33-43.
22. Andersson, K.; Malmqvist, P.-Å.; Roos, B. O.; Sadlej, A. J.; Wolinski, K. Second-Order Perturbation Theory with a CASSCF Reference Function. *J. Phys. Chem.* **1990**, *94*, 5483-5488.
23. Andersson, K.; Malmqvist, P.-Å.; Roos, B. O. Second-Order Perturbation Theory with a Complete Active Space Self-Consistent Field Reference Function. *J. Chem. Phys.* **1992**, *96*, 1218-1226.
24. de Graaf, C.; Broer, R.; Nieuwpoort, W. C. Comparison of the superexchange interaction in NiO and in a NiO [100] surface. *Chem. Phys. Lett.* **1997**, *271*, 372-376.
25. de Graaf, C.; Sousa, C.; Illas, F.; de P. R. Moreira, I. Magnetic interactions in biradicals, molecular complexes and ionic insulators: A comparison of the Difference Dedicated CI and CASPT2 methods. *Work in progress.* **2000**.
26. Andersson, K.; Blomberg, M. R. A.; Fülscher, M. P.; Karlström, G.; Lindh, R.; Malmqvist, P.-Å.; Neogrády, P.; Olsen, J.; Roos, B. O.; Sadlej, A. J.; Schütz, M.; Seijo, L.; Serrano-Andrés, L.; Siegbahn, P. E. M.; Widmark, P.-O. MOLCAS version 4, University of Lund, Sweden, 1997.
27. Maynau, D.; Ben Amor, N.CASDI suite of programs, Toulouse, 1997.
28. Illas, F.; de P. R. Moreira, I.; de Graaf, C.; Castell, O.; Casanovas, J. Absence of collective effects in Heisenberg systems with localized magnetic moments. *Phys. Rev. B.* **1997**, *56*, 5069-5072.
29. Okuda, K.; Noguchi, S.; Konishi, K.; Deguchi, H.; Takeda, K. Magnetism of one-dimensional copper oxides related to HTSC. *J. Magn. Magn. Mat.* **1992**, *104-107*, 817-818.
30. Martin, R. L.; Illas, F. Antiferromagnetic Exchange Interactions from Hybrid Density Functional Theory. *Phys. Rev. Lett.* **1997**, *79*, 1539-1542.